



Carbon Nanofibre Composites Decorated with Ru-Ag Nanophases for High-Efficiency Electrochemical Capacitors

Geon-Hyoung An and Hyo-Jin Ahn^z

Department of Materials Science and Engineering, Seoul National University of Science and Technology, Seoul 139-743, Korea

Composite electrodes made of carbon nanofibres (CNFs) decorated with Ru-Ag nanophases were synthesized through a combination of an electrospinning method and an impregnation method for use in high-efficiency electrochemical capacitors. The scanning electron microscopy (SEM), transmission electron microscopy (TEM), X-ray diffraction (XRD), and X-ray photoelectron spectroscopy (XPS) results indicate that the Ru-Ag nanophases are well decorated on the CNF electrode. The cyclic voltammetry (CV) results show that the CNF electrode decorated with Ru-Ag nanophases exhibits an excellent capacitance (≈ 350.0 F/g at 100 mV/s), superb high-rate capacitance in the range 10–200 mV/s, and excellent capacity retention ($\approx 98.6\%$).

© 2013 The Electrochemical Society. [DOI: 10.1149/2.005305ssl] All rights reserved.

Manuscript submitted November 9, 2012; revised manuscript received February 21, 2013. Published March 2, 2013.

Electrochemical capacitors have attracted considerable attention in various application fields (i.e., electric vehicles, flashlights, MP3 players) because of various advantages such as their high power density, high energy density, and long cycle life.^{1–3} In general, there are two different mechanisms for the operation of electrochemical capacitors. The first is electrical double-layer capacitance (EDLC) followed by a non-faradaic process. Activated carbon, carbon nanotubes, graphene, and carbon nanofibres (CNFs) have been used as EDLC electrode materials. The other mechanism is pseudo-capacitance followed by a faradaic process. RuO₂, IrO₂, MnO₂, and polymer electrodes are examples of pseudo-capacitance electrode materials.¹ Of the various oxide-based electrodes, RuO₂ has been studied extensively owing to its high specific capacitance (768 F/g). However, its disadvantages are its high cost, the aggregation of RuO₂ nanoparticles, and its relatively low electronic conductivity in high H₂O environments.^{4,5} Many technologies have been employed to overcome these disadvantages, including the use of CNF electrodes decorated with RuO₂. For example, Chuang et al. reported that RuO₂/CNF composites synthesized via a hydrothermal method showed a capacitance of 155 F/g at 200 mV/s and an excellent high-rate performance.⁵ Pico et al. investigated the electrochemical capacitance of RuO₂ deposited on CNF electrodes by using a catalytic vapor-growth procedure and an impregnation method.⁶ However, so far, there has been no study on CNF composite electrodes decorated with Ru and Ag nanophases for high-efficiency electrochemical capacitors. CNFs, fabricated by electrospinning, were chosen as the supporting materials because of their ease of fabrication, relatively low cost, and high electronic conductivity, as well as their use in EDLC electrodes.

In this work, we successfully synthesized composite electrodes of CNFs decorated with Ru-Ag nanophases by using an electrospinning method and an impregnation method, and investigated their electrochemical capacitor properties such as their capacitance, high-rate performance, and capacity retention.

Experimental

CNF composite electrodes decorated with Ru-Ag nanophases were prepared through a combination of an electrospinning method and an impregnation method. First, CNFs were fabricated by using a mixture solution of polyacrylonitrile (PAN, $M_w = 150,000$ g/mol, Aldrich) and poly(vinylpyrrolidone) (PVP, $M_w = 1,300,000$ g/mol, Aldrich) in *N,N*-dimethylformamide (DMF, Aldrich) for 5 h in the electrospinning process. For the fabrication of the CNFs, the potential and feeding rate were fixed at ≈ 13 kV and ≈ 0.03 mL/h, respectively. A 23-gauge needle was used, and the distance between the syringe tip and the fiber-collector was maintained at ≈ 15 cm. The as-spun nanofibres, consisting of PAN and PVP polymer composites, were stabilized by heating at 280°C for 5 h in an air atmosphere, and then

carbonized at 800°C for 3 h in nitrogen gas. The resulting CNFs were treated with a mixture solution (1:1 v/v) of HF and HNO₃ for 5 h to oxidize the carbon into COOH functional groups on their edge surfaces. Secondly, for the decoration of Ru-Ag nanophases on the CNFs, an impregnation method was used. The surface-oxidized CNFs were dispersed in deionized water by ultrasonication and stirring for 3 h. Then, RuCl₃ (Aldrich) and AgNO₃ (Aldrich) precursors were added to the dispersed solution. The amount of Ru precursor in the CNF was controlled to 20 wt%. The amount of Ag precursor was controlled so that Ru and Ag were in the molar ratio 8:2. NaBH₄ was used as the reducing agent for the synthesis of CNFs decorated with Ru and Ag nanophases. Subsequently, the decorated CNF composite electrodes were washed several times with deionized water, and then dried in an oven at 100°C for 3 h. For comparison, CNF electrodes decorated with only the Ru phase were synthesized using the above-described procedure. Thus, types of samples were produced for the electrochemistry tests: single CNF electrodes, CNF composite electrodes decorated with Ru nanophases, and CNF composite electrodes decorated with Ru and Ag nanophases (referred to herein as single CNF electrodes, sample A, and sample B, respectively).

The electrode morphologies and structures of all samples were characterized using field-emission scanning electron microscopy (FE-SEM; Hitachi S-4700) and transmission electron microscopy (TEM; JEOL, KBSI Suncheon Center). TEM-EDS elemental mapping of the samples was carried out using a Phillips CM20T/ STEM equipped with an energy-dispersive X-ray spectrometer (EDS). The crystal structures and chemical bonding states were analyzed using X-ray diffraction (XRD; Rigaku D/Max-2500 diffractometer equipped with a Cu K α source) and X-ray Photoelectron Spectroscopy (XPS; ESCALAB 250 equipped with an Al K α X-ray source). Electrochemical performance measurements were taken with a potentiostat/galvanostat (PGST302N by Eco Chemie, Netherlands) using a conventional three-electrode system consisting of a working electrode, a reference electrode, and a counter electrode. The working electrode was mixed with the as-prepared samples, acetylene black, and a polyvinylidene fluoride (PVDF) binder. The compositions of the mixture inks were controlled to a mass ratio of 7:2:1 in *N*-methyl-2-pyrrolidinone (NMP). The mixture inks of 3 μ L were loaded on the glassy carbon working electrode by a micropipette and then were dried at 70°C for 30 min. Ag/AgCl (sat. KCl) and Pt gauze were used as the reference and counter electrodes, respectively, and the electrolyte was 0.5 M H₂SO₄. The electrochemical performances of all samples were measured using cyclic voltammetry at scan rates of 10, 30, 50, 100, and 200 mV/s in the range 0.0–1.0 V.

Results and Discussion

Figure 1 shows the SEM images obtained from the single CNF electrode, sample A, and sample B. The images indicate that the diameters of the electrodes were in the approximate ranges

^zE-mail: hjahn@seoultech.ac.kr

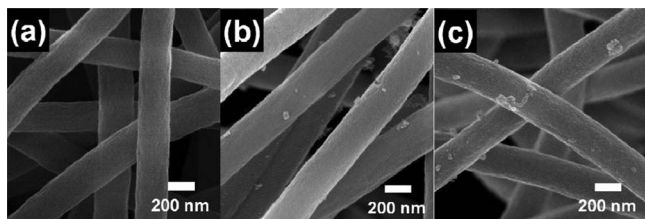


Figure 1. SEM images obtained from the single CNF electrode, sample A, and sample B. The diameters of the electrodes were in the approximate ranges 213–263 nm for the single CNF electrodes (a), 267–284 nm for sample A (b), and 243–280 nm for sample B (c), respectively.

213–263 nm for the single CNF electrodes, 267–284 nm for sample A, and 243–280 nm for sample B. The single CNF electrode showed a smooth electrode surface, but samples A and B showed rough surfaces on the CNF electrodes with a little aggregation of the nanophases, implying that Ru or Ru-Ag nanophases were formed on the surfaces of the CNF electrodes.

Figure 2 shows low-resolution TEM images ((a)–(c)) and high-resolution TEM images ((d)–(f)) of the single CNF electrode, sample A, and sample B. The single CNF electrode (Figure 2a and 2d) exhibited a uniform contrast region. However, the TEM images of samples A and B (Figure 2b and 2c) revealed nanosized dark blobs around the edge area of the CNF electrodes. That is, the high-resolution TEM results for sample A (Figure 2e) and sample B (Figure 2f) show that dark blobs (of $\approx 2\text{--}4$ nm in size) relative to the Ru nanophases or the Ru-Ag nanophases were decorated uniformly on the region of gray contrast relative to the CNF electrode. Furthermore, in the case of sample B, the Ru and Ag nanophases were not distinguished in the TEM images, as shown in Figure 2f. Thus, for a clear demonstration of the composition of the CNF electrodes decorated with Ru-Ag nanophases (sample B), TEM-EDS mapping measurements were performed as shown in Figure 3a–3d. The EDS results indicate that Ru and Ag atoms were uniformly distributed on the CNF electrodes. In this context, the excellent distribution of Ru-Ag nanophases could affect the electrochemical capacitor properties such as the electrochemical capacitance and high-rate performance.

Figure 4a shows the XRD data of the single CNF electrode, sample A, and sample B. The XRD pattern of single CNF electrode exhibits traditional diffraction peaks ($2\theta = 25^\circ$), indicating its general amorphous characteristics. For sample A, the pattern shows the main

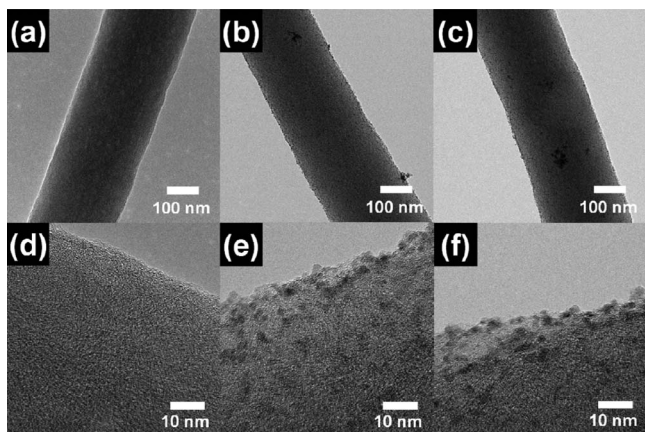


Figure 2. Low-resolution TEM images ((a)–(c)) and high-resolution TEM images ((d)–(f)) of the single CNF electrode, sample A, and sample B. The single CNF electrode (a) showed a uniform contrast region. The samples A and B ((b) and (c)) revealed nanosized dark blobs around the edge area of the CNF electrodes. The dark blobs (of $\approx 2\text{--}4$ nm in size) relative to the Ru nanophases or the Ru-Ag nanophases are shown in the high-resolution TEM images ((e) and (f)).

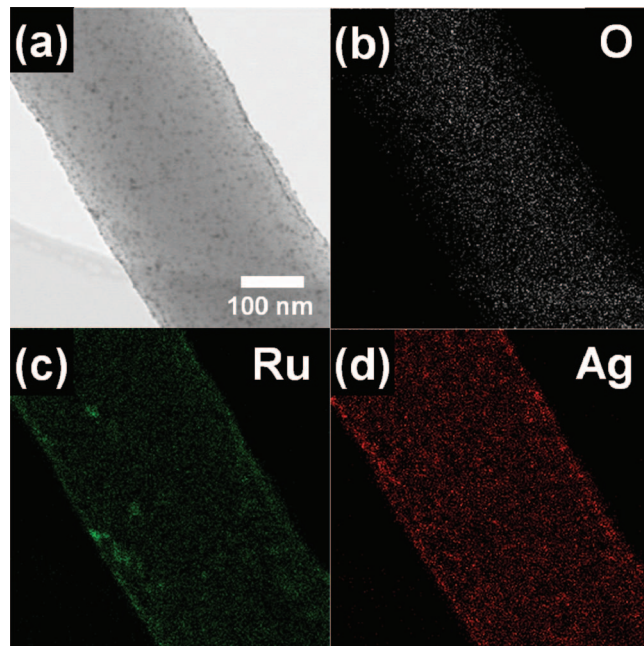


Figure 3. TEM-EDS mapping data obtained from sample B. STEM images for the sample B indicating CNF composite electrodes decorated with Ru and Ag nanophases is shown in the Figure 3(a). The mapping results reveal the uniform elemental distribution for O element (b), Ru element (c), and Ag element (d).

characteristic diffraction peaks at 38.4° , 42.1° , and 44.0° , corresponding to the (100), (002), and (101) planes, respectively [JCPDS card No. 06–0663]. This implies that the crystalline Ru nanophase has a hexagonal structure with the space group $P6_3/mmc$ [194]. For sample B, the pattern shows the main characteristic diffraction peak at 38.1° , corresponding to the (111) plane [JCPDS card No. 04–0783], implying that the crystalline Ag nanophase has the face-centered cubic structure with space group $Fm\bar{3}m$ [225]. In addition, the characteristic diffraction peaks of the abovementioned Ru nanophase are observed together. On the basis of the SEM, TEM-EDS, and XRD results, it

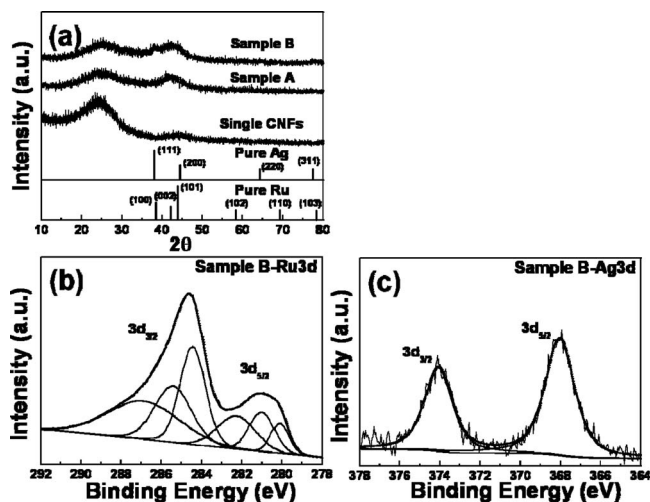


Figure 4. XRD plots obtained from the single CNF electrode, sample A, and sample B. The reference bulk reflections of pure Ru and Ag phases are shown in the bottom (JCPDS card No. 06–0663 and JCPDS card No. 04–0783). XPS spectra of (a) the Ru 3d and (b) Ag 3d core-levels obtained from sample B. The photoelectron energy of the Ru 3d and Ag 3d peaks were corrected by considering the reference C 1s peak at 284.5 eV.

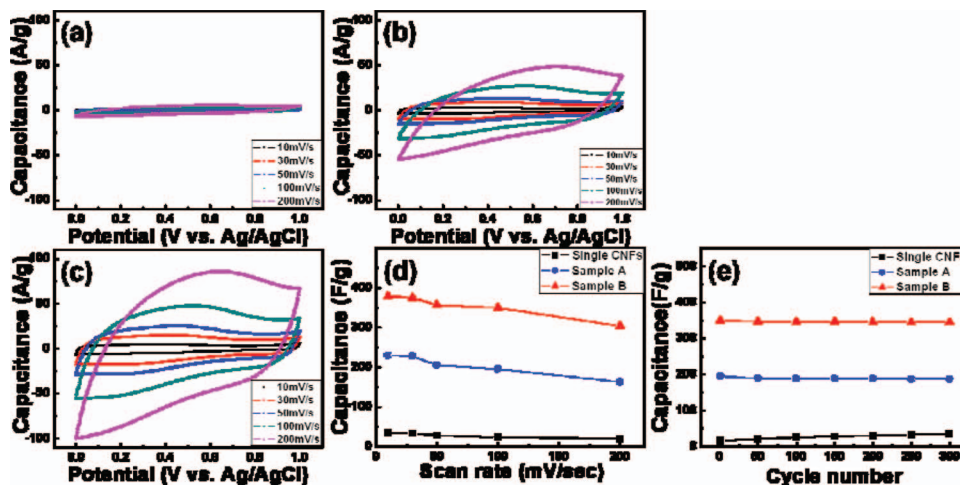


Figure 5. Cyclic voltammograms (CVs) of (a) the single CNF electrode, (b) sample A, and (c) sample B at scan rates of 10, 30, 50, 100, and 200 mV/s in the range 0.0–1.0 V. (d) Capacitance as a function of the potential scan rate calculated from the single CNF electrode, sample A, and sample B. (e) The cycle number dependence obtained from the single CNF electrode, sample A, and sample B up to 300 cycles, at a fixed scan rate of 100 mV/s.

is concluded that the electrode is composed of crystalline Ru and Ag composite nanophases decorated on the CNF electrodes. For the investigation of the chemical bonding states of Ru and Ag for sample B, XPS examinations were carried out. Figure 4b presents the XPS spectra of the Ru $3d_{3/2}$ and $3d_{5/2}$ photoelectrons. In particular, the Ru $3d_{3/2}$ spectral peak overlaps with the C 1s spectral peak (≈ 284.5 eV). Here, we considered only the Ru $3d_{5/2}$ spectral peak, that is, the XPS spectra for the Ru $3d_{5/2}$ photoelectrons consisted of three different signals observed at ≈ 280.0 and ≈ 281.0 eV, corresponding to the metallic Ru phase and RuO₂ phase, respectively.⁷ Considering the XRD and XPS results, it is concluded that the Ru phase is composed of a core region (metallic Ru states) and a shell region (mostly Ru oxide states). Furthermore, it is believed that the above Ru oxide phases could have a direct effect on the electrochemical capacitor performance. For the chemical bonding states of Ag, the XPS spectra of the Ag $3d_{3/2}$ and $3d_{5/2}$ photoelectrons are observed at ≈ 374.0 and ≈ 368.0 eV, implying that elemental Ag is present in the metallic Ag state.⁸

Figure 5a–5c shows cyclic voltammograms (CVs) for the single CNF electrode, sample A, and sample B, which were recorded at scan rates of 10, 30, 50, 100, and 200 mV/s in the range 0.0–1.0 V. The capacitances of all the samples were obtained using the following equation,^{9–11}

$$C = [q_a + q_c] / [2m\Delta V] \quad [1]$$

where q_a and q_c are the charges of the anodic and cathodic regions, respectively, and m and ΔV are the mass and potential range, respectively. The capacitances of the single CNF, sample A, and sample B are ≈ 22.9 , 195.6, and 350.0 F/g, respectively, at 100 mV/s, as shown in Figures 5a–5c. It is noteworthy that sample B (CNF composite electrode decorated with Ru-Ag nanophases) exhibits a superb capacitance performance compared to the single CNF and sample A. In particular, the capacitance of sample B is approximately 11 times higher than that of the single CNF electrode and around 1.8 times higher than that of sample A. These results indicate that the performance improvement can be attributed to the introduction of the well-dispersed Ru-Ag nanophase on the CNF electrodes. In other words, the reason for the enhancement may be that the presence of the Ag nanophase increases the conductivity of ions and electrons for the Ru nanophase and the CNF electrode. Furthermore, Figure 5d presents the high-rate performances of all the samples as a function of the capacitance versus the scan rates, as evaluated from Figure 5a–5c. The single CNF electrode, sample A, and sample B showed capacitances of ≈ 35.2 –19.3, ≈ 230.4 –162.5, and ≈ 378.5 –303.5 F/g, respectively, in the range 10–200 mV/s. In other words, the degradation efficiencies of the single CNF electrode, sample A, and sample B were $\approx 54.8\%$,

$\approx 70.5\%$, and $\approx 80.2\%$, respectively. Thus, sample B showed an excellent high-rate performance compared to the single CNF electrode and sample A because of the presence of the well-dispersed Ru-Ag nanophase. In other words, it is well-known that the relatively poor electronic conductivity of RuO₂ phases is directly related by the poor capacitive performance at high scan rates.⁴ Hence, introduction of the metallic Ru and Ag nanophases is influenced by the improved capacitive performance including high-rate performance owing to the enhanced conductivity of ions and electrons for electrodes in electrochemical capacitors. Therefore, it is possible that the CNF composite electrodes decorated with Ru-Ag nanophase can be applied as high-rate electrochemical capacitors. Figure 5e presents the cycle number dependence obtained from the single CNF electrode, sample A, and sample B up to 300 cycles, at a fixed scan rate of 100 mV/s. The capacity retention values for samples A and B are $\approx 96.0\%$ and 98.6% , respectively. Thus, all the samples exhibit superb capacity retention up to 300 cycles.

Conclusions

CNF composites decorated with Ru-Ag nanophases for use as electrodes in electrochemical capacitors were synthesized successfully via a combination of an electrospinning method and an impregnation method. Sample B gave an excellent capacitance (≈ 350.0 F/g at 100 mV/s), superb high-rate performance, and superb capacity retention (98.6%) compared to the single CNF electrode and sample A. This implies that CNF composite electrodes decorated with the Ru-Ag nanophases will be promising electrodes for use in high-efficiency electrochemical capacitors.

Acknowledgment

This research was supported by Basic Science Research Program through the National Research Foundation of Korea (NRF) funded by the Ministry of Education, Science and Technology (2012-007444).

References

1. B. E. Conway, *Electrochemical Supercapacitors*, p. 14, Klumer Academic Publishers, Norwell, MA (1999).
2. H.-J. Ahn, J. I. Sohn, Y.-S. Kim, H.-S. Shim, W. B. Kim, and T.-Y. Seong, *Electrochem Commun.*, **8**, 513 (2006).
3. H.-J. Ahn and T.-Y. Seong, *J. Alloys Compd.*, **478**, L8 (2009).
4. G.-L. Cui, X.-H. Zhou, L.-J. Zhi, T. Arne, and M. Klaus, *New Carbon Mater.*, **22**, 302 (2007).
5. C. M. Chung, C. W. Huang, H. Teng, and J. M. Ting, *Compos. Sci. Technol.*, (In Press) (2012).

6. F. Pico, J. Ibanez, M. A. Lillo-Rodenas, A. Linares-Solano, R. M. Rojas, J. M. Amarillar, and J. M. Rojo, *J. Power Sources*, **176**, 417 (2008).
7. R. Kotz, H. J. Lewerenz, and S. Stucki, *J. Electrochem. Soc.*, **130**, 825 (1983).
8. J. F. Moulder, W. F. Stickle, P. E. Sobol, and K. D. Bomben, *Handbook of X-ray Photoelectron Spectroscopy, Physical Electronics*, p. 121, Eden Prairie, MN (1995).
9. I.-H. Kim, J.-H. Kim, and K.-B. Kim, *Electrochem. Solid-State Lett.*, **8**, A369 (2005).
10. H.-J. Ahn, Y.-E. Sung, W. B. Kim, and T.-Y. Seong, *Electrochim. Solid-State Lett.*, **11**, A112 (2008).
11. J.-B. Lee, S.-Y. Jeong, W.-J. Moon, T.-Y. Seong, and H.-J. Ahn, *J. Alloys Compd.*, **509**, 4336 (2011).